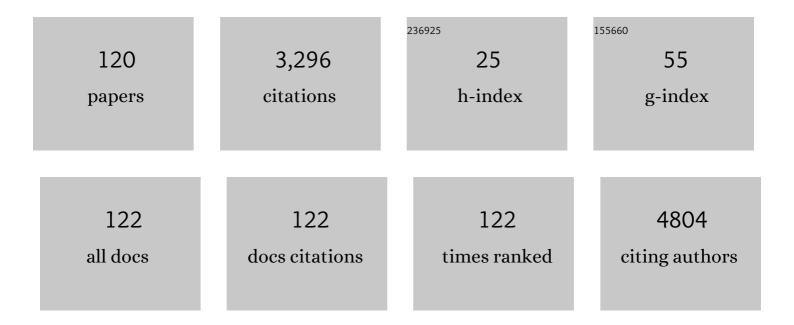
List of Publications by Year in descending order

Source: https://exaly.com/author-pdf/3906516/publications.pdf Version: 2024-02-01



#	Article	IF	CITATIONS
1	Growth of Ta ₂ SnO ₆ Films, a Candidate Wide-Band-Gap p-Type Oxide. Journal of Physical Chemistry C, 2022, 126, 3764-3775.	3.1	8
2	Urbach Energy and Open-Circuit Voltage Deficit for Mixed Anion–Cation Perovskite Solar Cells. ACS Applied Materials & Interfaces, 2022, 14, 7796-7804.	8.0	53
3	Impact of lifetime on the levelized cost of electricity from perovskite single junction and tandem solar cells. Sustainable Energy and Fuels, 2022, 6, 2718-2726.	4.9	11
4	Indium Gallium Oxide Emitters for High-Efficiency CdTe-Based Solar Cells. ACS Applied Energy Materials, 2022, 5, 5484-5489.	5.1	13
5	Tailoring the CdS/CdSe/CdTe multilayer structure for optimization of photovoltaic device performance guided by mapping spectroscopic ellipsometry. Solar Energy Materials and Solar Cells, 2021, 221, 110907.	6.2	8
6	Optical and Electronic Losses Arising from Physically Mixed Interfacial Layers in Perovskite Solar Cells. ACS Applied Materials & Interfaces, 2021, 13, 4923-4934.	8.0	14
7	Epitaxial stannate pyrochlore thin films: Limitations of cation stoichiometry and electron doping. APL Materials, 2021, 9, .	5.1	3
8	Protecting Perovskite Solar Cells against Moisture-Induced Degradation with Sputtered Inorganic Barrier Layers. ACS Applied Energy Materials, 2021, 4, 7571-7578.	5.1	20
9	Impact of Humidity and Temperature on the Stability of the Optical Properties and Structure of MAPbI3, MA0.7FA0.3PbI3 and (FAPbI3)0.95(MAPbBr3)0.05 Perovskite Thin Films. Materials, 2021, 14, 4054.	2.9	10
10	Mean Free Path of Photoelectronic Excitations in Hydrogenated Amorphous Silicon and Silicon Germanium Alloy Semiconductors. Physica Status Solidi (B): Basic Research, 2021, 258, 2000473.	1.5	0
11	Optical Properties of Magnesium-Zinc Oxide for Thin Film Photovoltaics. Materials, 2021, 14, 5649.	2.9	3
12	Optical properties of thin film Sb2Se3 and identification of its electronic losses in photovoltaic devices. Solar Energy, 2021, 228, 38-44.	6.1	11
13	Estimating Internal Stress of an Alteration Layer Formed on Corroded Boroaluminosilicate Glass through Spectroscopic Ellipsometry Analysis. ACS Applied Materials & Interfaces, 2021, 13, 50470-50480.	8.0	2
14	Glancing angle deposited CdTe: Nanostructured films and impact on solar cell performance. Surface and Coatings Technology, 2020, 381, 125127.	4.8	6
15	Real-Time Optimization of Anti-Reflective Coatings for CIGS Solar Cells. Materials, 2020, 13, 4259.	2.9	10
16	Low-bandgap mixed tin–lead iodide perovskites with reduced methylammonium for simultaneous enhancement of solar cell efficiency and stability. Nature Energy, 2020, 5, 768-776.	39.5	165
17	PERC silicon PV infrared to ultraviolet optical model. Solar Energy Materials and Solar Cells, 2020, 215, 110655.	6.2	6
18	Semi-transparent p-type barium copper sulfide as a back contact interface layer for cadmium telluride solar cells. Solar Energy Materials and Solar Cells, 2020, 218, 110764.	6.2	10

#	Article	IF	CITATIONS
19	Anisotropic Optical and Frictional Properties of Langmuir–Blodgett Film Consisting of Uniaxiallyâ€Aligned Rodâ€Shaped Cellulose Nanocrystals. Advanced Materials Interfaces, 2020, 7, 1902169.	3.7	12
20	Effects of intrinsic and atmospherically induced defects in narrow bandgap (FASnI3) <i>x</i> (MAPbI3)1â^ <i>x</i> perovskite films and solar cells. Journal of Chemical Physics, 2020, 152, 064705.	3.0	26
21	Characterization of chain alignment at buried interfaces using Mueller matrix spectroscopy. MRS Communications, 2020, 10, 292-297.	1.8	0
22	Non-contacting optical probing of photovoltaic device performance. , 2020, , .		1
23	Substrateâ€Dependent Molecular and Nanostructural Orientation of Nafion Thin Films. Advanced Functional Materials, 2019, 29, 1902699.	14.9	28
24	Irradiance and temperature considerations in the design and deployment of high annual energy yield perovskite/CIGS tandems. Sustainable Energy and Fuels, 2019, 3, 1841-1851.	4.9	30
25	n-i-p Nanocrystalline Hydrogenated Silicon Solar Cells with RF-Magnetron Sputtered Absorbers. Materials, 2019, 12, 1699.	2.9	6
26	Parametric Optical Property Database for CdSe1â^'xSx Alloys. Electronic Materials Letters, 2019, 15, 500-504.	2.2	6
27	Atmospherically induced defects in (FASnI ₃) _{0.6} (MAPbI _{3â^3<i>x</i>) Tj ETQq1 175102.}	1 0.784314 2.8	4 rgBT /Overla 7
28	Monolithic Two-Terminal All-Perovskite Tandem Solar Cells with Power Conversion Efficiency Exceeding 21%. , 2019, , .		3
29	Photogenerated Carrier Transport Properties in Silicon Photovoltaics. Scientific Reports, 2019, 9, 19015.	3.3	20
30	Reducing Saturationâ€Current Density to Realize Highâ€Efficiency Lowâ€Bandgap Mixed Tin–Lead Halide Perovskite Solar Cells. Advanced Energy Materials, 2019, 9, 1803135.	19.5	255
31	Emissivity of solar cell cover glass calculated from infrared reflectance measurements. Solar Energy Materials and Solar Cells, 2019, 190, 98-102.	6.2	19
32	Reducing Operating Temperature in Photovoltaic Modules. IEEE Journal of Photovoltaics, 2018, 8, 532-540.	2.5	68
33	Determination of conductivity anisotropy and the role of doping in single walled carbon nanotube thin films with THz spectroscopic ellipsometry. Carbon, 2018, 129, 592-597.	10.3	7
34	Optical simulation of external quantum efficiency spectra of Culn1â^Ga Se2 solar cells from spectroscopic ellipsometry inputs. Journal of Energy Chemistry, 2018, 27, 1151-1169.	12.9	10
35	Optical gradients in a-Si:H thin films detected using real-time spectroscopic ellipsometry with virtual interface analysis. Applied Surface Science, 2018, 436, 779-784.	6.1	1
36	Optical Evaluation of PERC Cell Reflectance for Thermal Management. , 2018, , .		0

#	Article	IF	CITATIONS
37	A Versatile Optical Model Applied to CdTe and CdSe <inf>1–y</inf> Te <inf>y</inf> Alloys: Sensitivity to Film Composition and Relative Defect Density. , 2018, , .		1
38	Efficient two-terminal all-perovskite tandem solar cells enabled by high-quality low-bandgap absorber layers. Nature Energy, 2018, 3, 1093-1100.	39.5	422
39	High Efficiency Ill–V Solar Cells. Springer Series in Optical Sciences, 2018, , 415-438.	0.7	0
40	Formamidinium + Cesium Lead Triiodide Perovskite Thin Films: Optical Properties and Devices. , 2018, , .		1
41	Glancing Angle Deposited CdTe: Optical Properties and Structure. , 2018, , .		1
42	Optical Hall Effect of PV Device Materials. IEEE Journal of Photovoltaics, 2018, 8, 1793-1799.	2.5	12
43	Formamidinium + cesium lead triiodide perovskites: Discrepancies between thin film optical absorption and solar cell efficiency. Solar Energy Materials and Solar Cells, 2018, 188, 228-233.	6.2	21
44	Real Time Spectroscopic Ellipsometry Analysis of First Stage Culn1â^'xGaxSe2 Growth: Indium-Gallium Selenide Co-Evaporation. Materials, 2018, 11, 145.	2.9	3
45	Optical and electrical properties of H2 plasma-treated ZnO films prepared by atomic layer deposition using supercycles. Materials Science in Semiconductor Processing, 2018, 84, 91-100.	4.0	12
46	Structural, optical, and hole transport properties of earth-abundant chalcopyrite (CuFeS2) nanocrystals. MRS Communications, 2018, 8, 970-978.	1.8	33
47	Optical properties of soda lime float glass from 3 mm to 148 nm (0.41 meV to 8.38 eV) by spec ellipsometry. Surface Science Spectra, 2018, 25, 016001.	troscopic	12
48	Spectroscopic ellipsometry study of thickness and porosity of the alteration layer formed on international simple glass surface in aqueous corrosion conditions. Npj Materials Degradation, 2018, 2, .	5.8	44
49	Understanding near infrared absorption in tin doped indium oxide thin films. Journal Physics D: Applied Physics, 2018, 51, 295302.	2.8	8
50	Spectroscopic ellipsometry determination of optical and electrical properties of aluminum doped zinc oxide. Applied Surface Science, 2017, 421, 852-858.	6.1	32
51	Spectroscopic ellipsometry for analysis of polycrystalline thin-film photovoltaic devices and prediction of external quantum efficiency. Applied Surface Science, 2017, 421, 601-607.	6.1	19
52	Optical properties of InP from infrared to vacuum ultraviolet studied by spectroscopic ellipsometry. Applied Surface Science, 2017, 421, 813-818.	6.1	7
53	Understanding and Eliminating Hysteresis for Highly Efficient Planar Perovskite Solar Cells. Advanced Energy Materials, 2017, 7, 1700414.	19.5	190
54	Morphological and optical properties of low temperature processed SnO ₂ :F. Physica Status Solidi (B): Basic Research, 2017, 254, 1700102.	1.5	9

#	Article	IF	CITATIONS
55	Al+Si Interface Optical Properties Obtained in the Si Solar Cell Configuration. Physica Status Solidi (A) Applications and Materials Science, 2017, 214, 1700480.	1.8	7
56	Nanostructure evolution of magnetron sputtered hydrogenated silicon thin films. Journal of Applied Physics, 2017, 122, .	2.5	10
57	Correlating the silicon surface passivation to the nanostructure of low-temperature a-Si:H after rapid thermal annealing. Journal of Applied Physics, 2017, 122, .	2.5	36
58	Optical response of mixed methylammonium lead iodide and formamidinium tin iodide perovskite thin films. AIP Advances, 2017, 7, .	1.3	24
59	Modification of reactively sputtered NiO _{<i>x</i>} thin films by pulsed UV laser irradiation. Physica Status Solidi (A) Applications and Materials Science, 2017, 214, 1600414.	1.8	13
60	Ellipsometric study of the optical response of ZnS:Cr for PV applications. Applied Surface Science, 2017, 421, 315-319.	6.1	3
61	Optical properties of borosilicate glass from 3.1 mm to 210 nm (0.4 meV to 5.89 eV) by spectr ellipsometry. Surface Science Spectra, 2017, 24, .	roscopic	10
62	Influence of Deposition Parameters on Silicon Thin Films Deposited by Magnetron Sputtering. , 2017, , .		0
63	Optical Properties of and Alloys and Their Application for CdTe Photovoltaics. , 2017, , .		6
64	Magnetron Sputtered Hydrogenated Silicon Thin Films: Assessment for Application in Photovoltaics. , 2017, , .		0
65	Electrical Transport Properties from Long Wavelength Ellipsometry. , 2017, , .		3
66	Application of Mapping Spectroscopic Ellipsometry for CdSe/CdTe Solar Cells: Optimization of Low-Temperature Processed Devices with All-Sputtered Semiconductors. , 2017, , .		0
67	Impact of Infrared Optical Properties on Crystalline Si and Thin Film CdTe Solar Cells. , 2017, , .		5
68	Spectroscopic Ellipsometry Studies of n-i-p Hydrogenated Amorphous Silicon Based Photovoltaic Devices. Materials, 2016, 9, 128.	2.9	7
69	Thermal Poling of Soda‣ime Silica Glass with Nonblocking Electrodes—Part 1: Effects of Sodium Ion Migration and Water Ingress on Glass Surface Structure. Journal of the American Ceramic Society, 2016, 99, 1221-1230.	3.8	55
70	Parameterized complex dielectric functions of CuIn 1â^'x Ga x Se 2 : applications in optical characterization of compositional nonâ€uniformities and depth profiles in materials and solar cells. Progress in Photovoltaics: Research and Applications, 2016, 24, 1200-1213.	8.1	34
71	Optical properties and degradation monitoring of CH <inf>3</inf> NH <inf>3</inf> PbI <inf>3</inf> . , 2016, , .		0
72	Culn <inf>1â^'x</inf> Ga <inf>x</inf> Se <inf>2</inf> solar cells with thin absorbers analyzed by spectroscopic ellipsometry: Insights into quantum efficiency and optical/collection losses. , 2016, , .		1

#	Article	IF	CITATIONS
73	LPCVD SiNx thin film on c-Si wafer by spectroscopic ellipsometry. Surface Science Spectra, 2016, 23, 51-54.	1.3	5
74	Effects of oxygen partial pressure, deposition temperature, and annealing on the optical response of CdS:O thin films as studied by spectroscopic ellipsometry. Journal of Applied Physics, 2016, 120, .	2.5	9
75	Optical monitoring of CH ₃ NH ₃ PbI ₃ thin films upon atmospheric exposure. Journal Physics D: Applied Physics, 2016, 49, 405102.	2.8	18
76	Breaking Malus' law: Highly efficient, broadband, and angular robust asymmetric light transmitting metasurface. Laser and Photonics Reviews, 2016, 10, 791-798.	8.7	38
77	Near infrared to ultraviolet anisotropic optical properties of single crystal SrLaAlO ₄ from spectroscopic ellipsometry. Physica Status Solidi (B): Basic Research, 2016, 253, 2066-2072.	1.5	4
78	Fabrication of Efficient Low-Bandgap Perovskite Solar Cells by Combining Formamidinium Tin Iodide with Methylammonium Lead Iodide. Journal of the American Chemical Society, 2016, 138, 12360-12363.	13.7	362
79	Near infrared to ultraviolet optical properties of bulk single crystal and nanocrystal thin film iron pyrite. Nanotechnology, 2016, 27, 295702.	2.6	14
80	Through-the-glass spectroscopic ellipsometry for analysis of CdTe thin-film solar cells in the superstrate configuration. Progress in Photovoltaics: Research and Applications, 2016, 24, 1055-1067.	8.1	54
81	Correlated metals as transparent conductors. Nature Materials, 2016, 15, 204-210.	27.5	291
82	Effect of molybdenum deposition temperature on the performance of CuIn1â^'xGaxSe2 Solar Cells. , 2015, , .		0
83	Quantum efficiency simulations with inputs from spectroscopic ellipsometry for evaluation of carrier collection in a-Si:H solar cells. , 2015, , .		2
84	Characterization of structure and growth evolution for nc-Si:H in the tandem photovoltaic device configuration. , 2015, , .		0
85	Optical properties of single-crystal Gd ₃ Ga ₅ O ₁₂ from the infrared to ultraviolet. Physica Status Solidi (B): Basic Research, 2015, 252, 2191-2198.	1.5	25
86	Through-the-glass spectroscopic ellipsometry for simultaneous mapping of coating properties and stress in the glass. , 2015, , .		0
87	Spectroscopic ellipsometry studies of CH3NH3PbX3 thin films and their growth evolution. , 2015, , .		5
88	High temperature coefficient of resistance molybdenum oxide and nickel oxide thin films for microbolometer applications. Optical Engineering, 2015, 54, 037101.	1.0	13
89	Spectroscopic Ellipsometry Applied in the Full p-i-n a-Si:H Solar Cell Device Configuration. IEEE Journal of Photovoltaics, 2015, 5, 307-312.	2.5	11
90	Characterization of Structure and Growth Evolution for nc-Si:H in the Tandem Photovoltaic Device Configuration. IEEE Journal of Photovoltaics, 2015, 5, 1516-1522.	2.5	3

#	Article	IF	CITATIONS
91	Real-Time, In-Line, and Mapping Spectroscopic Ellipsometry for Applications in Cu(In \$_{{f 1}-{m) Tj ETQq1 1 0.7	84314 rgB 2.5	T ∤Qverlock
92	Optical properties of single crystal Bi4Ge3O12 from the infrared to ultraviolet. Journal of Applied Physics, 2014, 116, .	2.5	13
93	Investigation of doped a-Si <inf>1−x</inf> C <inf>x</inf> :H as a novel back contact material for CdTe solar cells. , 2014, , .		2
94	High-Speed Imaging/Mapping Spectroscopic Ellipsometry for In-Line Analysis of Roll-to-Roll Thin-Film Photovoltaics. IEEE Journal of Photovoltaics, 2014, 4, 355-361.	2.5	29
95	Applications of real-time and mapping spectroscopic ellipsometry for process development and optimization in hydrogenated silicon thin-film photovoltaics technology. Solar Energy Materials and Solar Cells, 2014, 129, 32-56.	6.2	19
96	Optical Monitoring and Control of Three-Stage Coevaporated Cu(In \$_{m {1-x}}\$Ga\$_{m x}\$)Se \$_{f 2}\$ by Real-Time Spectroscopic Ellipsometry. IEEE Journal of Photovoltaics, 2013, 3, 375-380.	2.5	8
97	Large-Area Compositional Mapping of Cu(In\$_{1-x}\$Ga \$_{x}\$)Se \$_{2}\$ Materials and Devices with Spectroscopic Ellipsometry. IEEE Journal of Photovoltaics, 2013, 3, 359-363.	2.5	35
98	Large nonlinear optical coefficients in pseudo-tetragonal BiFeO3 thin films. Applied Physics Letters, 2013, 103, .	3.3	32
99	Growth evolution of Si:H prepared with SiH <inf>4</inf> + Si <inf>2</inf> H <inf>6</inf> as studied by real time spectroscopic ellipsometry. , 2013, , .		0
100	Effect of reduced dimensionality on the optical band gap of SrTiO3. Applied Physics Letters, 2013, 102, .	3.3	52
101	Correlations Between Mapping Spectroscopic Ellipsometry Results and Solar Cell Performance for Evaluations of Nonuniformity in Thin-Film Silicon Photovoltaics. IEEE Journal of Photovoltaics, 2013, 3, 387-393.	2.5	19
102	Band gap and structure of single crystal Bil3: Resolving discrepancies in literature. Journal of Applied Physics, 2013, 114, .	2.5	109
103	Effect of c-Si doping density on heterojunction with intrinsic thin layer (HIT) radial junction solar cells. , 2013, , .		2
104	Multichannel spectroscopic ellipsometry for CdTe Photovoltaics: From real-time monitoring to large-scale mapping. , 2013, , .		0
105	Electrical properties of plasma enhanced chemical vapor deposition a-Si:H and a-Si1â ^{~3} xCx:H for microbolometer applications. Journal of Applied Physics, 2013, 114, 183705.	2.5	19
106	Correlations between mapping spectroscopic ellipsometry results and solar cell performance for evaluations of nonuniformity in thin-film silicon photovoltaics. , 2013, , .		0
107	Optical monitoring and control of three-stage coevaporated Cu(In <inf>1−x</inf> Ga <inf>x</inf>)Se <inf>2</inf> by real-time spectroscopic ellipsometry. , 2013, , .		0
108	Large-area compositional mapping of Cu(In <inf>1−x</inf> Ga <inf>x</inf>)Se <inf>2</inf> materials and devices with spectroscopic ellipsometry. , 2013, , .		0

#	Article	IF	CITATIONS
109	Correlations between mapping spectroscopic ellipsometry results and solar cell performance for evaluations of nonuniformity in thin-film silicon photovoltaics. , 2012, , .		0
110	Conformational Effects of Adsorbed Polymer on the Swelling Behavior of Engineered Clay Minerals. Clays and Clay Minerals, 2012, 60, 363-373.	1.3	8
111	Large-area compositional mapping of Cu(In <inf>1−x</inf> Ga <inf>x</inf>)Se <inf>2</inf> materials and devices with spectroscopic ellipsometry. , 2012, , .		0
112	Optical monitoring and control of three-stage coevaporated Cu(In <inf>1−x</inf> Ga <inf>x</inf>)Se <inf>2</inf> by real-time spectroscopic ellipsometry. , 2012, , .		12
113	Single wall carbon nanotube electrodes for hydrogenated amorphous silicon solar cells. , 2012, , .		4
114	High Energy Density, High Temperature Capacitors Utilizing <scp><scp>Mn</scp></scp> â€Doped <scp><scp>0.8CaTiO₃–0.2CaHfO₃</scp></scp> Ceramics. Journal of the American Ceramic Society, 2012, 95, 1348-1355.	3.8	111
115	Low Temperature Crystallization of Metastable Nickel Manganite Spinel Thin Films. Journal of the American Ceramic Society, 2012, 95, 2562-2567.	3.8	22
116	Fabrication and optimization of single-junction nc-Si:H n–i–p solar cells using Si:H phase diagram concepts developed by real time spectroscopic ellipsometry. Journal of Non-Crystalline Solids, 2008, 354, 2397-2402.	3.1	17
117	Analysis of Compositionally and Structurally Graded Si:H and Si1â^xGex:H Thin Films by Real Time Spectroscopic Ellipsometry. Materials Research Society Symposia Proceedings, 2008, 1066, 1.	0.1	3
118	Advanced Deposition Phase Diagrams for Guiding Si:H-Based Multijunction Solar Cells. Materials Research Society Symposia Proceedings, 2007, 989, 2.	0.1	2
119	Dielectric Functions of a-Si _{1-x} Ge _x :H versus Ge Content, Temperature, and Processing: Advances in Optical Function Parameterization. Materials Research Society Symposia Proceedings, 2006, 910, 1.	0.1	11
120	Surface Roughening Transition in Si _{1-x} Ge _x :H Thin Films. Materials Research Society Symposia Proceedings, 2006, 910, 2.	0.1	2